



ELSEVIER

Contents lists available at ScienceDirect

Opto-Electronics Review

journal homepage: <http://www.journals.elsevier.com/opto-electronics-review>

Disorder-induced natural quantum dots in InAs/GaAs nanostructures

A. Babiński

Faculty of Physics, University of Warsaw, ul. Pasteura 5, 02-093, Warszawa, Poland

ARTICLE INFO

Article history:

Received 27 October 2017
 Received in revised form 29 January 2018
 Accepted 19 February 2018
 Available online 3 March 2018

Keywords:

Quantum dots
 Optical properties

ABSTRACT

Properties of excitons confined to potential fluctuations due to indium distribution in the wetting layer which accompany self-assembled InAs/GaAs quantum dots are reviewed. Spectroscopic studies are summarized including time-resolved photoluminescence and corresponding single-photon emission correlation measurements. The identification of charge states of excitons is presented which is based on results of a theoretical analysis of interactions between the involved carriers. The effect of the dots' environment on their optical spectra is also shown.

© 2018 Association of Polish Electrical Engineers (SEP). Published by Elsevier B.V. All rights reserved.

Contents

1. Introduction.....	73
2. Basic properties of natural quantum dots in the InAs/GaAs wetting layer.....	74
3. The environment effect on the natural quantum dots.....	77
4. Conclusions.....	78
Acknowledgements.....	78
References.....	78

1. Introduction

A quantum confinement of carriers in semiconductor structures is a basic concept used in many electronic and optoelectronic applications. Two-dimensional confinement in quantum wells (QWs) or at heterointerfaces has been employed in electronics for years. Quantum dots (QDs), which have been studied and applied in semiconductor physics for more than 20 years [1], provide an insight into properties of strongly interacting carriers confined in all three directions. The confinement in QDs can be characterized by the relative strength of Coulomb interactions between involved carriers and the confinement energy. A strong confinement is provided, e.g., in self-assembled QDs when the former energy is lower or comparable to the latter one. A weak confinement is provided when the Coulomb interaction is stronger than the quantum confinement.

The weak quantum confinement is observed in several semiconductor systems. Isolated objects, which can confine excitons, can be formed by a local interdiffusion of a GaAs/AlGaAs QW structure induced by laser light [2]. Seminal are studies on excitons

confined in thin QWs grown with interruptions at the interfaces [3,4]. Well-defined atomic steps at the interface provide a lateral confinement of carriers and the resulting potential landscape leads to characteristic properties of weakly confined excitons. The weak confinement was also observed in thin QWs which were grown with no interruption at the structure heterointerfaces [5]. The distribution of atomic species at the interfaces results in potential fluctuations responsible for the carrier confinement in those structures. The weak confinement was also observed in several other systems as, e.g., the QDs formed by selective interdiffusion in CdTe/CdMgTe QWs [6] or InGaAs/GaAs quantum dashes [7].

Properties of yet another system are reviewed in this work. It was shown that excitons can be confined to natural QDs (WLQDs), which emerge in the wetting layer (WL) – thin layer of QDs material which is present in structures together with self-assembled InAs/GaAs QDs [8]. The confinement of carriers in all three dimensions in those WLQDs is provided by fluctuations of potential energy related to fluctuations of indium composition in the WL [8]. It is shown in the following that excitons confined to the fluctuations possess all the properties of electron-hole complexes confined to QDs.

E-mail address: babinski@fuw.edu.pl

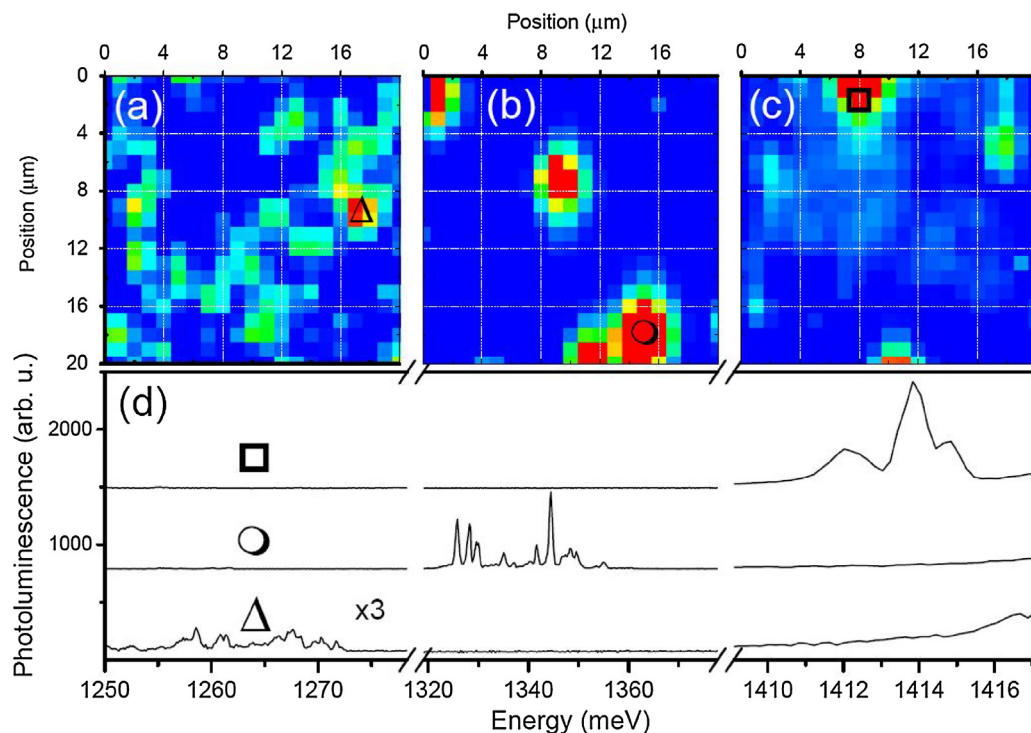


Fig. 1. The colour-coded maps of the micro-PL integrated over (a) 1.25 eV–1.278 eV; (b) 1.319 eV–1.378 eV; (c) 1.409 eV–1.417 eV. The energy regions correspond to the emission from self-assembled InAs/GaAs QDs, not fully grown QDs, and WLQDs, respectively. The spectra collected from specific regions of the sample are presented in Fig. 1(d).

2. Basic properties of natural quantum dots in the InAs/GaAs wetting layer

A WL accompanies self-assembled QDs grown in a Stranski-Krastanow mode. Substantial difference in the InAs and GaAs lattice constants results in a formation of a strongly strained thin InAs layer on which coherent InAs islands spontaneously grow [9,10]. Such a simple picture gets complicated in real systems as subsequent steps in the growth procedure can result in significant segregation of In atoms as well as In/Ga intermixing which is further promoted by the strain in the structure. The degree of the intermixing is affected by growth details. As a result, a non-symmetric shape of the In composition profile along the growth direction can be observed in some cases. This is related to segregation of indium atoms which takes place during the structure growth. The profile can be characterized by using a phenomenological Muraki model of indium segregation [11]. It was shown in Ref. [12] that the composition of the WL is also modulated in lateral direction which results in a rather complicated potential energy landscape depending on all three dimensions. The indium fraction in the WL was shown to reach the level of 0.35–0.40 while in other areas the fraction was equal to around 0.2. Regions of an increased In composition are about 2–3 nm large. As a result of the fluctuations excitons can be confined to some regions of the WL.

The fluctuations were observed in several InAs/GaAs structures with self-assembled QDs grown by MBE using an “in-flush” technique [13]. A crucial step in the technique is a growth interruption before the self-assembled QDs are fully covered with a GaAs barrier. As a result, flat self-assembled QDs are achieved with a relatively low inhomogeneous broadening of the corresponding emission energy. Results presented in this work were obtained on a structure with a single layer of InAs QDs grown on a 600 nm undoped GaAs buffer layer. The In-flush procedure was applied at 5 nm and the dots were capped with a 100 nm GaAs layer. The size of the excitation spot on the sample employed in experimental setups for micro-photoluminescence (micro-PL) studies was usually kept

below 1 μm. For some experiments a structure with mesas of sizes from 1 μm to 20 μm was employed in order to reproducibly locate the same dot for several measurements. The sample annealed for 30 s at 850°C was also studied to observe the effect of thermal annealing on the properties of the dots.

The spatial distribution of the fluctuations can be appreciated by inspection of the micro-PL from the sample area of 20 × 20 μm² as presented in a colour-coded map in Fig. 1. Fig. 1(a)–(c) correspond to the integrated PL from energy ranges related to self-assembled QDs, not fully-grown QDs (most likely QDs completely covered before the In-flush procedure), and WLQDs, respectively. The spectra collected from three different points at the sample, which are presented in Fig. 1(d), as well as the maps confirm that the emission from those three objects is not spatially correlated. The self-assembled QDs provide a strong confinement to charge carriers. As a result, the optical emission can be observed in the energy range below approx. 1.3 eV. Properties of excitons and multiexcitons confined in those QDs were presented elsewhere [14–16]. The emission in the intermediate energy range (1.319 eV–1.378 eV) was not studied previously. The emission due to excitons confined to WLQDs can be observed in the energy range of 1.409 eV–1.417 eV. Separate, sharp emission lines can be detected in the energy range, slightly below the energy of the WL emission.

A limited spectral resolution of the experimental setup used to obtain results of Fig. 1 prevents a more detailed analysis of the WLQD emission. Focusing on the energy range of interest one can find the characteristic pattern of main emission lines due to single WLQDs. When excited with relatively low power density, the spectrum usually consists of two emission lines. These lines are denoted in Fig. 2(a) with X and X⁺. The increase of excitation power density results in the increase of their intensity [see Fig. 2(b)]. Moreover, an additional emission line (2X) appears in the spectrum at lower energy. At the highest excitation power density the 2X feature is dominant. Excitation–power dependencies of the three lines intensities allow to establish a multiplicity of involved excitons. A close

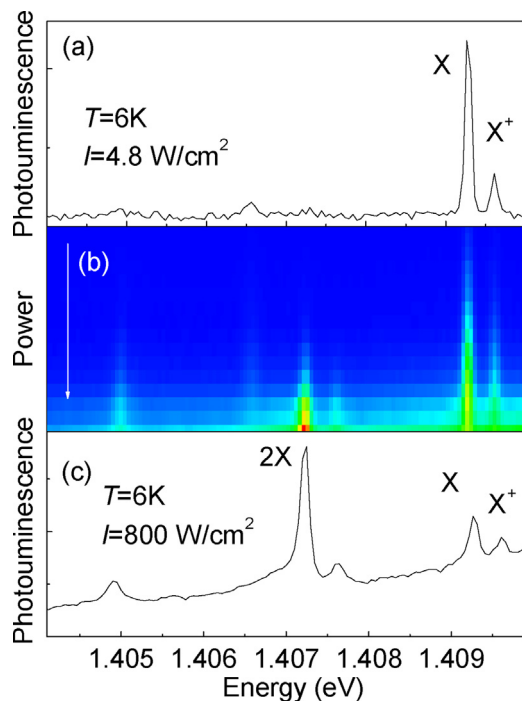


Fig. 2. Emission from a single WLQD at $T=6\text{K}$ excited with low (a) and high (c) excitation power density. Evolution of the spectrum with increasing power is also shown - (b).

to linear (a power law $n=0.8\text{--}0.9$) dependence of the X and X^+ lines suggests their correspondence to a complex comprising single exciton. The intensity of the 2X line increases superlinearly with the excitation power density – the corresponding exponent of the power law equals $n=1.55$. This points to the attribution of the 2X line to the recombination of a complex comprising two excitons. In order to establish the charge state of the excitons, PL studies with polarization sensitivity were performed. It was found that the X and 2X emission lines comprise two components. Both components of each feature are linearly polarized in perpendicular directions (see Fig. 3). The energy difference between the components depend on the investigated dot but it was hardly higher than $20\ \mu\text{eV}$. Moreover, in the case of a single dot, the sign of the X emission line splitting is opposite to the sign of the 2X emission line splitting. The splitting results from an anisotropic exchange interaction in the investigated electron-hole complex. For the X emission line the splitting corresponds to an electron-hole exchange in the initial state of transition which is a neutral exciton (electron-hole pair). The initial configuration of a neutral biexciton consists of two electrons and two holes in spin-singlet configurations, therefore the exchange interaction disappears. The final state of a 2X transition is an exciton. Therefore, the splitting of 2X transition is opposite to the splitting of X transition which can be seen in Fig. 3. The splitting pattern observed in the experiment confirms the attribution of X and 2X emission lines to neutral excitons and biexcitons in the WLQD. The optically distinguished directions of the sample, correspond to $[110]$ and $[1\bar{1}0]$ crystallographic directions of the substrate. This confirms the expected elongation of localization potential wells along one of those axes. The non-equivalence is due to anisotropic diffusion coefficient of ad-absorbed indium atoms on the $[100]$ GaAs surface [17], which takes place during the sample growth. The optical asymmetry was not observed for the X^+ emission line. This corresponds to its attribution to the recombination of a trion (charged exciton) in the WLQD. The trion initial state comprises a spin-singlet pair of excess carriers in which no exchange interaction is involved. The observation of both emission due to recombination of neutral excitons and trions in the PL spectrum (compare Fig. 3) is

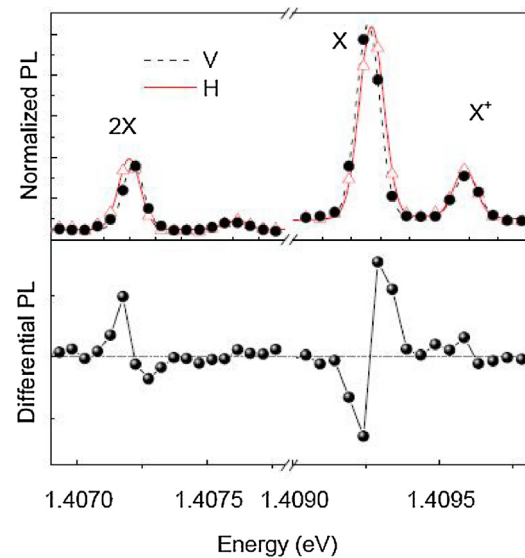


Fig. 3. Normalized polarization-sensitive micro-PL spectra of the excitons localized in a single WLQD (upper panel). The circles and triangles correspond to experimental points for the vertical and horizontal linear polarizations of detected light, respectively. The dotted and full lines are Gaussian fits of the corresponding spectra. The difference between the intensities of the horizontally and vertically polarized emission is shown with points in the lower panel.

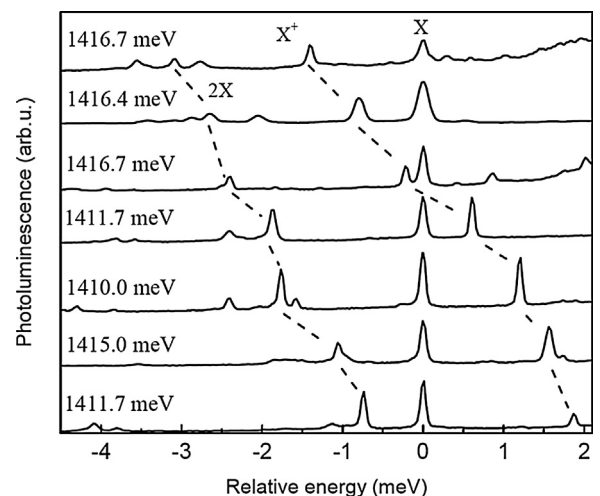


Fig. 4. Photoluminescence spectra of several WLQDs with neutral exciton (X), biexciton (2X), and positive trion (X^+) emission lines. Measurements are taken at $T=1.6\text{K}$. The energy scale is relative to the exciton emission energy for each spectrum. The directions of the sample, which are optically distinguished.

very often reported in studies of QDs [18] excited non-resonantly and reflects fluctuations of the QDs charge state over a timescale of an experiment. In the case of the WLQDs' a characteristic pattern of the spectra can be recognized. It can be appreciated in Fig. 4 that the binding energy of the biexciton (which is energy difference between 2X and X features in spectrum) substantially changes from dot to dot. Simultaneously, the energy difference between 2X and X^+ emission lines is constant (being of the order of $2\text{--}2.5\text{meV}$). The constant energy difference and the substantial variation of biexciton binding energy results sometimes in the shift of X^+ emission line energy above the energy of X emission line. This behaviour was studied in more details in Ref. 19. It was shown, using atomistic calculations, that the scattering in biexciton binding energies results mainly from random fluctuations of actual In atoms distribution. Energy appears to be a very sensitive function of the lattice randomness. At the same time, it practically does not depend on

exciton energy. The substantial distribution of biexciton and the positive trion binding energies is accompanied by the correlation of their relative energies. The variety of different random realizations of a single WLQD leads in some cases to the reversal of excitonic lines' order. As a result, positive trion energy can exceed neutral exciton energy. The quantitative trend for several indium atoms distribution samples used for atomistic calculations in Ref. 19 was explained in terms of several involved electron-hole Coulomb integrals. It was shown that the electron-electron repulsion integral did not change substantially when different random realizations were considered. This is related to a large delocalization of electronic wavefunction and its small susceptibility to random lattice fluctuations. Holes are typically more localized than electrons and the highly spatially-variable biaxial strain substantially affects their confining potential. Therefore, the hole-hole repulsion Coulomb integral is a sensitive function of alloying effects. Both biexciton and trion binding energies are affected in a similar way. Another interesting result of the calculations concerns the excited energy states of carriers confined to WLQDs. It was found that just electron and hole ground states could be explicitly classified as WLQD states. This is related to their substantial energy separation from the rest of the WL continuum, rather than the spatial localization. This conclusion also corresponds to the observed lack of any clear experimental manifestation of the excited states' occupation. Another point to be made is the attribution of the observed trion to the positively charged exciton. This may be explained in terms of the expected background acceptor presence in GaAs layers, which are not doped intentionally. The usual presence of positive triions in the spectrum is also consistent with a larger probability to be localized by potential fluctuations for holes than for electrons. Holes are heavier as compared to electrons, which explains the fact. It must be noted that although the positive trion is usually observed in the spectra of single WLQDs, a negatively charged exciton can be sometimes present, as it will be discussed later in the text. Finally, it is to be noted that similar trend of the positive trion energy following the biexciton energy can be also observed in, e.g., self-assembled InAs/GaAs QDs [20], CdTe/ZnTe QDs [21], and strain-free GaAs/GaAlAs QDs [22].

Time-dependent measurements of the emission from the WLQDs were also performed. Lifetimes of single carrier complexes in the WLQDs are equal to 0.57 ns–0.85 ns. A shorter lifetime of 0.39 ns was observed for the neutral biexciton 2X line [23]. The lifetimes are in average 2 times shorter than those observed for arrays of self-assembled InAs/GaAs QDs from the same sample, which were equal to approx. 1.6 ns. The relatively short lifetime of excitonic complexes confined to WLQDs was referred to the weak confinement of carriers in those objects. One may note that the efficient carrier recombination in the WLQDs has also implications for the performance of optoelectronic devices. Lateral carrier transport in the WL, which feeds the QDs may be affected by trapping electrons and holes in the WLQDs [24]. The lower efficiency of QD feeding with carriers may deteriorate the performance of possible optoelectronic devices.

The dynamics of the excitation transfer within the WLQD-WL system was also studied in annealed (30 s at 850 °C) structures with WLQDs [25]. In accordance with the single-dot measurements on the as-grown structure, the experimental data from the annealed structure can be modeled using the lifetime of the ground (WLQDs) state equal to 0.53 ± 0.03 ns. Within the model based on nonlinear rate equations, when the WLQDs are fully occupied (saturated), the states of higher energy decay slowly, mainly by radiative recombination. Later, with empty (due to recombination) WLQDs, the decay accelerates as carriers can relax non-radiatively to the WLQDs. The lifetime of the WL states (when the WLQDs are full) equals 1.1 ± 0.2 ns and the internal relaxation time (when the ground states are empty) equals 0.07 ± 0.01 ns.

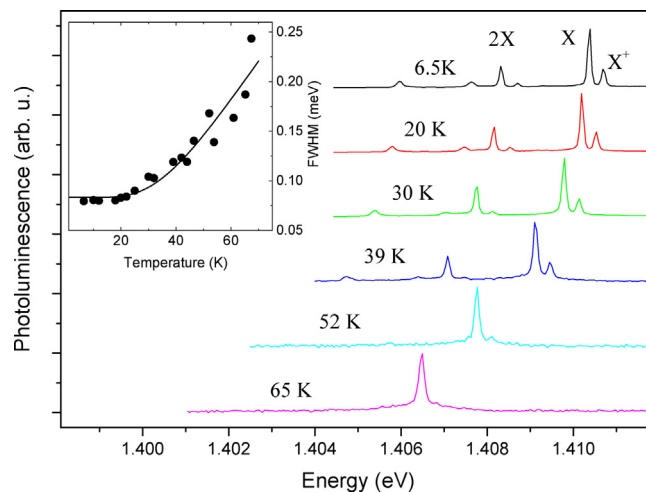


Fig. 5. Temperature dependence of the micro-PL spectra normalized at the neutral exciton (X) emission for a fixed excitation intensity. In the inset: temperature dependence of PL line width of the neutral exciton (X) and a fit of the form $\Gamma(T) = \Gamma_0 + A \exp(-E_A/kT)$, with $\Gamma_0 = 0.08$ meV, and the activation energy $E_A = 12 \pm 2$ meV.

Another characteristic property of WLQDs is the corresponding non-classical single photon emission. This confirmation of the single photon emission was provided by means of photon correlation measurements [23]. A well-pronounced suppression of a central ($t=0$) peak can be observed in autocorrelation of the X line, which is related to the photon antibunching effect. The relative height of the central peak reaches a second-order correlation parameter of $g^{(2)}(t=0) = 0.16 \pm 0.07$. The obtained $g^{(2)}(t=0)$ parameter compared with its threshold value of 0.5 confirms the single-photon emission from the dots. This is also confirmed by the observed cascade-type cross-correlation between 2X and X emission. The peak, which corresponds to the subsequent emission of 2X and X photons, was more pronounced than an average peak by a factor of $g^{(2)}(t=0) = 2.5 \pm 0.2$. This is related to the relatively strong excitation regime used in the experiment. Finally, interesting effects recorded for the X-X* cross-correlation between neutral and charge excitons can be addressed. For both the negatively charged and the positively charged excitons, the height of peaks around the central one in the correlation histograms exhibited an asymmetry, characteristic of the single-carrier capture mechanism [26].

The emission from single WLQDs was also studied at temperatures higher than 5 K [27]. The results are consistent with the attribution of X and X* (originally related to charged exciton) to neutral and positively charged exciton, respectively. It was observed (see Fig. 5) that the X* emission line disappeared from the spectrum at $T \sim 50$ K, while the X emission line was observed at temperatures up to 70 K. The quenching of X* emission at lower temperature than quenching of the X emission arises from the enhanced probability of an excess carrier escape from the ground state to higher energy states [28–31]. Temperature-dependent PL measurements also revealed the broadening of the emission lines as a function of temperature. FWHM of the X emission line did not change significantly up to $T = 20$ K (see inset to Fig. 5). At higher temperatures the emission line broadened. The broadening correlates with a decrease in the emission intensity which indicates that thermal activation of carriers to higher energy states was responsible for the broadening. The temperature dependence of the X emission line-broadening can be reasonably well reproduced with a formula: $\Gamma(T) = \Gamma_0 + A \exp(-E_A/kT)$ [28] with $\Gamma_0 = 0.08$ meV, and the activation energy $E_A = 12 \pm 2$ meV (see inset to Figure). The activation energy most likely corresponds to the phonon-induced activation of a carrier from the ground state to the excited state.

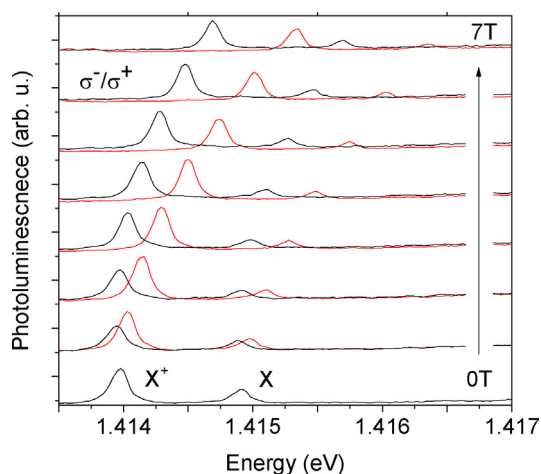


Fig. 6. The emission from a single WLQDs in magnetic field. Red (black) lines represent σ^- (σ^+) polarized spectra. (For interpretation of the references to colour in this figure legend, the reader is referred to the web version of this article.)

Properties of the WLQDs were also investigated in magnetic field. The evolution of the emission lines from WLQD in the Faraday configuration of the field was studied in Ref. 32. Results of measurements with polarization sensitivity performed in the configuration are presented in Fig. 6. The excitonic emission lines split in magnetic field into two components of circular polarization and shift their emission to higher energies. In moderate magnetic fields the dispersion of X excitonic emission lines can be expressed as:

$$E(B) = E(0) \pm \frac{1}{2} g^* \mu_B B + \gamma B^2 \quad (1)$$

The second term in the equation is related to energy splitting between two components of the bright exciton ($|M| = 1$) of opposite momenta. Splitting is due to the Zeeman interaction of the spin with external magnetic field. The Zeeman splitting between excitons' components is a linear function of magnetic field. This observation proves that excitons in the WLQDs comprise mainly electrons and heavy holes. Such a structure of excitons corresponds to the significant splitting between heavy and light-hole valence subbands due to the strain accommodated in WL. The effective g^* -factors corresponding to the splitting vary substantially from dot to dot ($g^* = 1.1$ – 2.2) [32,33,34]. The variation of the g^* -factors may be related to the actual distribution of In atoms in WLQD [10]. This corresponds to the effective g^* -factors in III–V QDs, which can substantially vary depending on strain, geometry, and confinement. The quadratic diamagnetic shift (γB^2) of the emission energy with the magnetic field was observed in the low-field regime. The diamagnetic coefficient γ varies from dot to dot and it is of the order of 10 – $20 \mu\text{eV}/\text{T}^2$. The values are similar to those found for GaAs/AlGaAs thin QWs [4]. Using typical electron ($0.053m_0$) and heavy-hole ($0.153m_0$) mass [35] – an approximation of the excitonic radius can be done. Resulting size is of the order of 4 – 6 nm , which corresponds to the size of In-regions of the WL (2 – 3 nm), as observed in TEM analysis of the investigated structure [12]. As long as cyclotron energy of the exciton in WLQD is smaller than the exciton binding energy, the magnetic-field dependence of the exciton energy is dominated by the diamagnetic shift. In higher fields the dependence deviates from quadratic towards linear evolution characteristic of Landau level quantization.

3. The environment effect on the natural quantum dots

At the advent of interest in physics of QDs they were usually called “artificial atoms” which emphasized their resemblance to atoms in which electrons are confined in the potential of a nucleus.

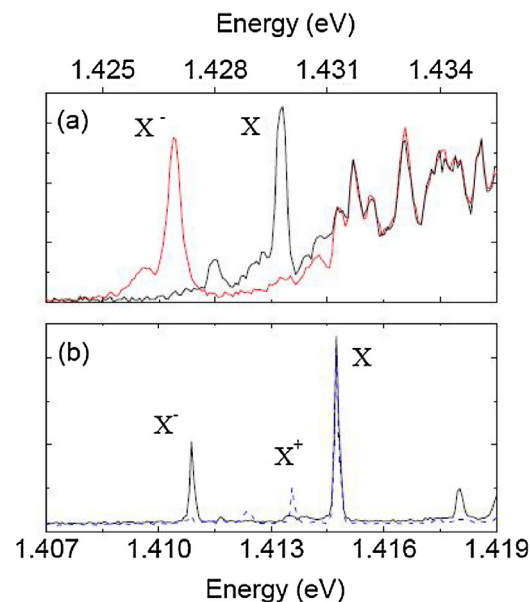


Fig. 7. Single-dot photoluminescence spectra of WLQDs: (a) the effect of high intensity excitation and (b) the excitation energy ($4.2 \mu\text{W}$ @ $\lambda = 760 \text{ nm}$ – continuous line and $4.2 \mu\text{W}$ @ $\lambda = 760 \text{ nm} + 40 \text{ nW}$ @ $\lambda = 650 \text{ nm}$ – dashed line) on the WLQDs charge state.

It is very well known now that such a picture is far from being justified. Interactions of carriers confined to QDs with atoms, which form the dots, as well as their interaction with environment are making the physics of QDs still a very interesting topic of studies.

The environment effect on electronic properties of confined carriers was also observed in WLQDs. The attribution of the trion which follows the biexciton with a constant energy difference to the positive charge state also allows for attribution of the other trion, sometimes present in the spectra, to the negative charge state. Observation of one or the other charge state substantially depends on excitation and the local environment of WLQD. Examples of such a dependence are shown in Fig. 7. The thermally annealed sample (850°C for 30 s) with WLQDs with mesas was employed in the experiment [36]. The In/Ga intermixing in that sample results in the blue-shift of the emission from WLQDs [37]. It was observed that the high excitation intensity resulted in a metastable change of the spectrum [see Fig. 6(a)]. While the lineshape of the emission from WL (which reflects the fluctuations of its composition) does not change upon the cycling, the low-energy emission lines corresponding to WLQDs do. It was observed that the X^- feature disappeared and another emission line X emerged at higher energy. Difference between the two configurations was confirmed by the measurements in magnetic field. While the X emission line split in two components, the X^- was found to split in magnetic field into four components. The quadruplet splitting of the emission line from a WLQD, which was also observed in the as-grown structure [38], was attributed to the spin-triplet configuration of a negatively charged dot. If the relaxation (combined with a spin-flip) of the electron from the excited state is blocked by excess carriers, the spin-triplet trion recombination takes place leaving the extra electron in the excited state. The splitting between the spin-singlet and the spin-triplet trions emerges in magnetic field. This explains the apparent quadruplet splitting of the emission line [39].

The charge state of a WLQD also depends on the energy of the excitation laser line. Two spectra shown in Fig. 7(b) were obtained with a femtosecond, pulsed $\lambda = 760 \text{ nm}$ excitation (continuous line) and a combined $\lambda = 760 \text{ nm}$ accompanied by a weak $\lambda = 650 \text{ nm}$ excitation – (dashed line) [23]. The spectrum changes considerably after an additional higher-energy excitation is added. The rela-

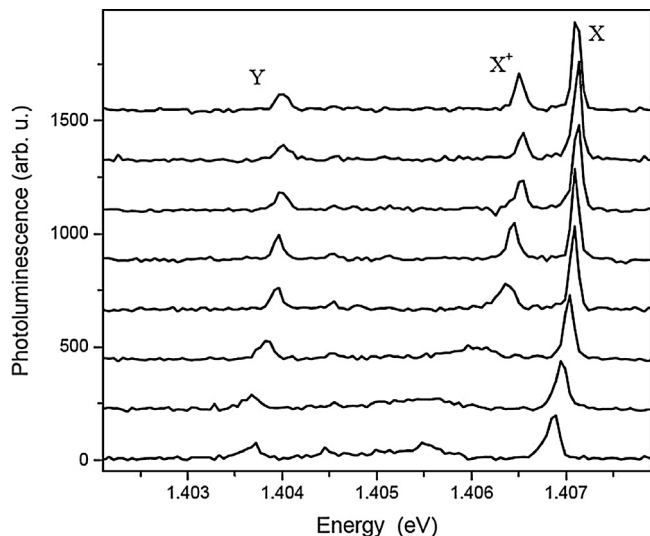


Fig. 8. Spectra from a single WLQD in a mesa subject to random fluctuations of electric field in the structure. The spectra (from top to bottom) were collected subsequently with 1 s collection time.

tively weak higher-energy excitation (with 100 times lower power density than simultaneous low-energy excitation) must affect the charge environment of the dot resulting in the modified spectrum. The main observed change is the quenching of the negative trion (X^-) accompanied with the emergence of a positively charged exciton (X^+). While the charged state of the WLQD can be controlled by the excitation conditions, excitons in WLQDs can be also affected by random fluctuations of the dot environment. An example of such an effect is shown in Fig. 8. A series of spectra recorded (with 1 s. accumulation time) from a mesa with WLQDs are shown in the Figure. The presented integrated spectra were recorded immediately one after another, which allows to appreciate timescale of the changes. It can be seen that the spectra substantially change in time. The changes must result from uncontrolled changes of the WLQD environment. The X emission line red-shift corresponds to quantum-confined Stark shift of the excitonic energy level in the increasing electric field. The red-shift is accompanied by the asymmetric broadening of the emission line. Even more substantial is the broadening of the positive trion X^+ which almost completely disappears from the spectrum. The most likely explanation of the observed effects involves many-body interactions of the excitons with a Fermi sea of electrons in a vicinity of the dot. The tunneling between electronic state in the dot and the density of states of delocalized electrons results in the broadening of the emission. The asymmetric broadening of the most red-shifted X emission reflects in this model the electron distribution around the Fermi level in the sea of electrons in the vicinity of the dot. Similar effects were observed in structures with the controlled potential distribution between QDs and a doped back contact [40]. The random character of the spectrum fluctuations makes their more detailed analysis rather difficult, however its possible origin may be related to charge fluctuations at the side-walls of the investigated mesa structure.

4. Conclusions

Properties of WLQDs which form in InAs/GaAs WL are reviewed. Basic characteristics of the neutral and charged excitons confined to the WLQDs is presented. It is shown that the energy of the biexcitonic transition ($2X$) follows the trion energy. The attribution of the charged exciton to the positive trion based on atomistic calculations of the WLQDs microscopic structure is discussed. Time-resolved micro-PL measurements reveal the single-photon emission from

WLQDs. The observed fast recombination of excitons in WLQDs may affect transport of carriers in optoelectronic devices, which employ self-assemble QDs. Effects of the dot environment on the properties of excitons confined in the WLQDs are also presented. The properties correspond to those of excitons in QDs in the weak confinement regime.

Acknowledgements

The work is partially supported by the Polish Funds for Science 2015. The author is grateful to all co-authors of the referenced papers on WLQDs, who largely contributed to the understanding of the physics involved. Acknowledged is a kind permission of A. Golnik and T. Kazmierczuk to use their results in Figs. 1 and 7, respectively.

References

- [1] G.W. Bryant, G. Salomon, *Optics of Quantum Dots and Wires*, Artech House Boston, 2005.
- [2] K. Brunner, U. Bockelmann, G. Abstreiter, M. Walther, G. Böhm, G. Tränkle, G. Weimann, Photoluminescence from a single GaAs/AlGaAs quantum dot, *Phys. Rev. Lett.* 69 (1992) 3216.
- [3] D. Gammon, E.S. Snow, B.V. Shanabrook, D.S. Katzer, D. Park, Fine structure splitting in the optical spectra of single GaAs quantum dots, *Phys. Rev. Lett.* 76 (1996) 3005.
- [4] L. Besombes, K. Kheng, D. Martrou, Exciton and biexciton fine structure in single elongated islands grown on a vicinal surface, *Phys. Rev. Lett.* 85 (2000) 425.
- [5] M. Erdman, C. Ropers, M. Wenderoth, R.G. Ulbricht, S. Malzer, G.H. Döhler, Diamagnetic shift of disorder-localized excitons in narrow GaAs/AlGaAs quantum wells, *Phys. Rev. B* 74 (2006) 125412.
- [6] S.V. Zaitsev, M.K. Welsch, A. Forchel, G. Bacher, Excitons in artificial quantum dots in the weak spatial confinement regime, *J. Exp. Theor. Phys.* 105 (2007) 1241.
- [7] G. Sek, A. Musiał, P. Podemski, M. Syperek, J. Misiewicz, A. Löffler, S. Höfling, L. Worschech, A. Forchel, Exciton kinetics and few particle effects in self-assembled GaAs-based quantum dashes, *J. Appl. Phys.* 107 (2010) 096106.
- [8] M. Hugues, M. Teisseire, J.-M. Chauveau, B. Vinter, B. Damilano, J.-Y. Duboz, J. Massies, Optical determination of the effective wetting layer thickness and composition in InAs/Ga(In) as quantum dots, *Phys. Rev. B* 76 (2007) 075335.
- [9] J.-Y. Marzin, J.-M. Gérard, A. Izraël, D. Barrier, G. Bastard, Photoluminescence of single InAs quantum dots obtained by self-organized growth on GaAs, *Phys. Rev. Lett.* 73 (1994) 716.
- [10] L. Goldstein, F. Glas, J.Y. Marzin, M.N. Charasse, G. Le Roux, Growth by molecular beam epitaxy and characterization of InAs/GaAs strained-layer superlattices, *Appl. Phys. Lett.* 47 (1985) 1099.
- [11] K. Muraki, S. Fukatsu, Y. Shiraki, Surface segregation of In atoms during molecular beam epitaxy and its influence on the energy levels in InGaAs/GaAs quantum wells, *Appl. Phys. Lett.* 61 (1992) 557.
- [12] A. Babiński, J. Borysiuk, S. Kret, M. Czyż, A. Golnik, S. Raymond, Z.R. Wasilewski, Natural quantum dots in the InAs/GaAs wetting layer, *Appl. Phys. Lett.* 92 (2008) 171104.
- [13] Z.R. Wasilewski, S. Fafard, J.P. McCaffrey, Size and shape engineering of vertically stacked self-assembled quantum dots, *J. Cryst. Growth* 201–202 (1999) 1131.
- [14] M. Vachon, S. Raymond, A. Babiński, J. Lapointe, Z. Wasilewski, M. Potemski, Energy shell structure of a single InAs/GaAs quantum dot with a spin-orbit interaction, *Phys. Rev. B* 79 (2009) 165427.
- [15] S. Awirothananon, S. Raymond, S. Studenikin, M. Vachon, W. Render, A. Sachrajda, X. Wu, A. Babiński, M. Potemski, S. Fafard, S.J. Cheng, M. Korkusinski, P. Hawrylak, Single-exciton energy shell structure in InAs/GaAs quantum dots, *Phys. Rev. B* 78 (2008) 235313.
- [16] A. Babiński, M. Potemski, S. Raymond, J. Lapointe, Z. Wasilewski, Fock-Darwin spectrum of a single InAs/GaAs quantum dot, *Phys. Status Solidi (c)* 3 (2006) 3748.
- [17] H. Nakamura, S. Kohmoto, T. Ishikawa, K. Asakawa, Novel nano-scale site-controlled InAs quantum dot assisted by scanning tunneling microscope probe, *Phys. E* 7 (2000) 331.
- [18] J.J. Finley, A.D. Ashmore, A. Lemaitre, D.J. Mowbray, M.S. Skolnick, I.E. Itskevich, P.A. Maksym, M. Hopkinson, T.F. Krauss, Charged and neutral exciton complexes in individual self-assembled In(Ga)As quantum dots, *Phys. Rev. B* 63 (2001) 073307.
- [19] M. Zieliński, K. Gołasa, M.R. Molas, M. Goryca, T. Kazmierczuk, T. Smolenski, A. Golnik, P. Kossacki, A.A.L. Nicolet, M. Potemski, Z.R. Wasilewski, A. Babiński, Excitonic complexes in natural InAs/GaAs quantum dots, *Phys. Rev. B* 91 (2015) 085303.
- [20] M.-F. Tsai, H. Lin, C.-H. Lin, S.-D. Lin, S.-Y. Wang, M.-Lo, S.-J. Cheng, M.-C. Lee, W.-H. Chang, Diamagnetic response of exciton complexes in semiconductor quantum dots, *Phys. Rev. Lett.* 101 (2008) 267402.

- [21] T. Kazimierczuk, T. Smolenski, M. Goryca, Ł. Kłopotowski, P. Wojnar, K. Fronc, A. Golnik, M. Nawrocki, J.A. Gaj, P. Kossacki, Magnetophotoluminescence study of intershell exchange interaction in CdTe/ZnTe quantum dots, *Phys. Rev. B* 84 (2011) 165319.
- [22] M. Abbarchi, T. Kuroda, T. Mano, K. Sakoda, C.A. Mastrandrea, A. Vinatteri, M. Gurioli, T. Tsuchiya, Energy renormalization of exciton complexes in GaAs quantum dots, *Phys. Rev. B* 82 (2010) 201301.
- [23] T. Kazimierczuk, A. Golnik, P. Kossacki, J.A. Gaj, Z.R. Wasilewski, A. Babiński, Single-photon emission from the natural quantum dots in the InAs/GaAs wetting layer, *Phys. Rev. B* 84 (2011) 115325.
- [24] E.S. Moskalenko, M. Larsson, W.V. Schoenfeld, P.M. Petroff, P.O. Holtz, Carrier transport in self-organized InAs/GaAs quantum-dot structures studied by single-dot spectroscopy, *Phys. Rev. B* 73 (2006) 155336.
- [25] K.P. Korona, A. Babiński, S. Raymond, Z. Wasilewski, Dynamics of excitation transfer inside InAs/GaAs quantum dot system, *Acta Phys. Pol. A* 110 (2006) 219.
- [26] J. Suffczyński, T. Kazimierczuk, M. Goryca, B. Piechal, A. Trajnerowicz, K. Kowalik, P. Kossacki, A. Golnik, K.P. Korona, M. Nawrocki, J.A. Gaj, G. Karczewski, Excitation mechanisms of individual CdTe/ZnTe quantum dots studied by photon correlation spectroscopy, *Phys. Rev. B* 74 (2006) 085319.
- [27] A. Babiński, M. Czyż, J. Borysiuk, S. Kret, A. Golnik, S. Raymond, J. Lapointe, Z.R. Wasilewski, Neutral and charged excitons localized in the InAs/GaAs wetting layer, *Acta Phys. Pol. A* 114 (2008) 1055.
- [28] R. Oulton, A.I. Tartakovskii, A. Ebbens, J. Cahill, J.J. Finley, D.J. Mowbray, M.S. Skolnick, M. Hopkinson, Temperature-induced carrier escape processes studied in absorption of individual $\text{In}_x\text{Ga}_{1-x}\text{As}$ quantum dots, *Phys. Rev. B* 69 (2004) 155323.
- [29] F. Olbrich, J. Kettler, M. Bayerbach, M. Paul, J. Höschel, S.L. Portalupi, M. Jetter, P. Michler, Temperature-dependent properties of single long-wavelength InGaAs quantum dots embedded in a strain reducing layer, *J. App. Phys.* 121 (2017) 184302.
- [30] L. Besombes, K. Kheng, L. Marsal, H. Mariette, *Phys. Rev. B* 63 (2001) 155307.
- [31] M. Bayer, A. Forchel, Temperature dependence of the exciton homogeneous linewidth in $\text{In}_{0.60}\text{Ga}_{0.40}\text{As}/\text{GaAs}$ self-assembled quantum dots, *Phys. Rev. B* 65 (R) (2002) 041308.
- [32] A. Babiński, A. Golnik, J. Borysiuk, S. Kret, P. Kossacki, J.A. Gaj, S. Raymond, M. Potemski, Z. Wasilewski, Three-dimensional localization of excitons in the InAs/GaAs wetting layer—magneto spectroscopic study, *Phys. Status Solidi (b)* 246 (2009) 850.
- [33] K. Gołasa, M. Molas, M. Goryca, T. Kazimierczuk, T. Smoleński, M. Koperski, A. Golnik, P. Kossacki, M. Potemski, Z.R. Wasilewski, A. Babiński, Properties of excitons in quantum dots with a weak confinement, *Acta Phys. Pol. A* 124 (2013) 781.
- [34] R. Kotlyar, T.L. Reinecke, M. Bayer, A. Forchel, Zeeman spin splittings in semiconductor nanostructures, *Phys. Rev. B* 63 (2000) 085310.
- [35] P.P. Paskov, P.O. Holtz, B. Monemar, J.M. Garcia, W.V. Schoenfeld, P.M. Petroff, Magnetoluminescence of highly excited InAs/GaAs self-assembled quantum dots, *Phys. Rev. B* 62 (2000) 7344.
- [36] A. Babiński, M. Potemski, S. Raymond, Z.R. Wasilewski, Charged and neutral excitons in natural quantum dots in the InAs/GaAs wetting layer, *Phys. E* 40 (2008) 2078.
- [37] A. Babiński, J. Jasiński, R. Bożek, A. Szepielow, J.M. Baranowski, Rapid thermal annealing of InAs/GaAs quantum dots under a GaAs proximity cap, *Appl. Phys. Lett.* 79 (2001) 2576.
- [38] A. Babiński, S. Raymond, Z. Wasilewski, J. Lapointe, M. Potemski, Localization of excitons in the wetting layer accompanying self-assembled InAs/GaAs quantum dots, *Acta Phys. Pol. A* 105 (547) (2006).
- [39] M. Bayer, G. Ortner, O. Stern, A. Kuther, A.A. Gorbunov, A. Forchel, P. Hawrylak, S. Fafard, K. Hinzer, T.L. Reinecke, S.N. Walck, J.P. Reithmaier, F. Klopff, F. Schäfer, Fine structure of neutral and charged excitons in self-assembled $\text{In}(\text{Ga})\text{As}/(\text{Al})\text{GaAs}$ quantum dots, *Phys. Rev. B* 65 (2002) 195315.
- [40] N.A.J.M. Kleemans, J. van Bree, A.O. Govorov, J.G. Keizer, G.J. Hamhuis, R. Nötzel, A. Yu. Silov, P.M. Koenraad, Many-body exciton states in self-assembled quantum dots coupled to a Fermi sea, *Nat. Phys.* 6 (2010) 534.